

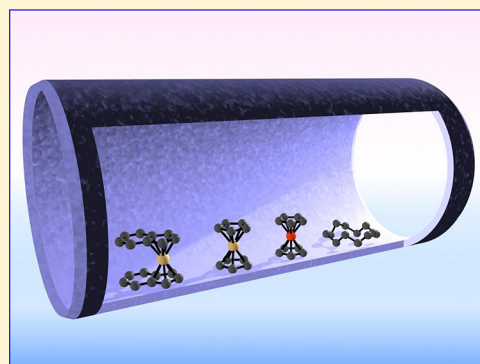
Adsorption of Ruthenium and Iron Metallocenes on Silica: A Solid-State NMR Study

Kyle J. Cluff, Nattamai Bhuvanesh, and Janet Blümel*

Department of Chemistry, Texas A&M University, P.O. Box 30012, College Station, Texas 77842-3012, United States

Supporting Information

ABSTRACT: Ruthenocene, bis(indenyl)ruthenium, bis(tetrahydroindenyl)ruthenium, cyclododecane, ferrocene, and ferrocene- d_2 have been adsorbed on silica surfaces by grinding the polycrystalline materials with silica. The adsorption process proceeds without solvent and is practically complete within 2 h. Its progress is monitored by ^1H , ^{13}C , and ^2H solid-state NMR spectroscopy. The transition from the crystal lattice to the surface species that are highly mobile is proven by strongly reduced chemical shift anisotropies and diminished dipolar interactions. Furthermore, the residual line widths are reduced. All solid-state NMR spectra indicate that the transition from a monolayer to the crystalline state is abrupt, and no multiple layers form on the surfaces. A correlation between surface coverage and ^2H residual line widths has been established. Besides a hydrophobic dry silica surface, wet and TMS-capped silica have been used as supports. The adsorption leads to the highest surface coverages and most mobile species for the surface of rigorously dried silica. The ^2H MAS spectra of surface-adsorbed ferrocene- d_2 prove that the motion of the metallocenes on the surfaces is fast and nearly isotropic, as in solution. Consequently, it is demonstrated that ^1H and ^{13}C NMR spectra of adsorbed ferrocene can be recorded using a conventional liquids NMR instrument.



I. INTRODUCTION

Metallocenes and their derivatives constitute an important substance class, and they are indispensable components in wide-ranging areas spanning from catalysis to stereoselective synthesis. Surprisingly, however, their surface chemistry on oxides, such as silica, is basically unexplored. This is astonishing because chromocene, for example, reacts with silica and alumina to generate the Union Carbide polymerization catalyst.^{1,2} Furthermore, chromatography, using original or modified silica, is the standard purification method for metallocenes.

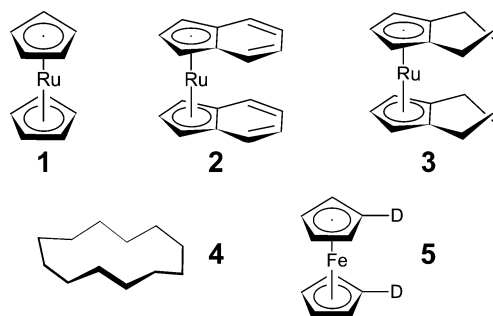
In general, the key step leading to reactions with surfaces or chromatographic purification is adsorption, a noncovalent, reversible interaction with the surface. Therefore, we strive to deepen our insights into the adsorption process. Our strategy hereby is twofold. We first need to develop a better understanding about the nature of compounds that can be adsorbed versus those that are not adsorbed. For this purpose a rough screening using different compounds with and without aromatic systems is indispensable. Second, we have to investigate the behavior of adsorbed molecules on the surface. Disentangling and quantifying the different modes of mobility of the surface species will significantly enhance our understanding in this respect. ^2H solid-state NMR of a deuterated surface-adsorbed compound will be investigated for this purpose.

We have recently reported on two representative metallocenes, chromocene and ferrocene, and demonstrated that

both are adsorbed on a silica surface and in this way become highly mobile, although their melting points are rather high (ferrocene: 172–174 °C, chromocene: 168–170 °C).³ It has been found that, besides the impregnation method, dry grinding of the components without a solvent led to the same outcome.

In this contribution it will be demonstrated using the substances 1–5 (Scheme 1), besides Cp_2Fe , that the adsorption, and ensuing mobility, of the metallocenes is a universal phenomenon, and new insights into surface adsorption processes and the dynamics of the adsorbed molecules will be presented. Cp_2Ru (1) shows that a larger

Scheme 1. Molecules Used for Adsorption on Silica Surfaces



Received: March 10, 2014

Published: May 7, 2014

central metal, and therefore distance between the Cp rings, does not impede the mobility on the surface. (Ind)₂Ru (2) allows probing whether an extended aromatic system is still able to adsorb on the nonplanar surface of amorphous silica. With (Ind-H₄)₂Ru (3) the effect of the deviation of the aromatic ligand from planarity on the adsorption is investigated. The question whether polarity of a species plays a role in its adsorption characteristic is answered by adsorbing cyclododecane (4) on silica. In order to study the different modes of mobility and to obtain a first estimate about the reorientation time of the surface-adsorbed species, deuterated ferrocene (5) is applied (Scheme 1).

Academic studies are usually conducted using model systems with planar surfaces, and most of the surface techniques employed for their characterization are invasive or provide only fragmentary data on specific functional groups, such as IR. Other techniques are not practical for the swift throughput of large numbers of samples. Solid-state NMR spectroscopy,⁴ on the other hand, provides deep insight into adsorption phenomena. It is not invasive and allows detecting and quantifying dynamic scenarios besides giving structural information about the species interacting with the surface. The early research by Günther^{5,6} showed that the narrowing of the ¹³C MAS signals is observed for a variety of adsorbed polycyclic aromatic hydrocarbons (PAHs).^{5,6} When adsorption occurs, the $\delta(^{13}\text{C})$ of the NMR signal changes, and the half-widths and chemical shift anisotropies (CSA)^{4b} of the ¹H and ¹³C MAS resonances are reduced.^{5,6} The analogous effects have been verified by our preliminary work with ferrocene and chromocene.³ With ¹H, ¹³C, and ²H MAS NMR we will describe how the adsorption and the ensuing mobilities of the adsorbed surface species 1a–5a, derived from dry grinding of the polycrystalline substances 1–5 with different silica supports, manifest themselves. The results are expected to have far-reaching implications, for example, for catalytic reaction mechanism studies on surfaces, and they should lead to a better insight into solid–solid interactions.

Besides initial investigations,^{3,5,6} all adsorption studies have been performed with volatile adsorbates and mostly on metal surfaces. This literature is voluminous, and for the sake of brevity and clarity we exclude this area here. However, some representative adsorption studies with high-melting substances in related fields are mentioned.

(a) Phosphine oxides⁷ and phosphines⁸ have been applied to probe acidic sites on surfaces by ³¹P solid-state NMR. Most of the adsorbed phosphines⁸ display high mobility on oxide surfaces. This is proven, among other means, by the cross-polarization (CP) characteristics^{4d,8,9} of the ³¹P CP/MAS resonances.

(b) Adsorbed polycyclic aromatic hydrocarbons (PAH) with higher melting points can show high mobility on different oxide surfaces.^{5,6,10} It has been proven that the NMR investigation of adsorbed PAHs can be especially revealing. For example, there are significant ¹³C chemical shift changes for the adsorbed as compared to the polycrystalline state, but also the large intrinsic ¹³C CSA^{4a} of the PAHs is reduced due to their higher mobility on the surface. Even substituents and functional groups are tolerated, as in the case of the carbonyl group in benzophenone or the halides in 1,4-dibromonaphthalene.⁵ It has been described additionally that fullerenes adsorb on mesoporous silica (MCM-41) upon dry grinding of the components.¹¹ The ¹³C resonances shift upon adsorption,^{5,6} and therefore this

process has to be based on the interaction of the π electrons with the surface. This interaction persists in the case where Fe and Cr are sandwiched between the aromatic Cp ligands.³ Therefore, the main goal is to investigate whether changing the electronics and geometry of the metallocenes by choosing the larger Ru as the center metal will have a measurable effect on their adsorption.

Here, it is investigated whether the adsorption characteristics of PAH, ferrocene, and chromocene on surfaces^{5,6,10} of mesoporous oxide materials will be found in the organometallics ruthenocene (1), bis(indenyl)ruthenocene (2), and its hydrogenated version 3 (Scheme 1) when adsorbed on silica to give 1a, 2a, and 3a. In order to check whether purely aliphatic molecules show the adsorption effects, cyclododecane (4) is applied, and for quantifying the modes of mobility, the deuterated ferrocene 5 (Scheme 1) is adsorbed on silica. In contrast to chromocene^{2a,b} the species 1–5 are diamagnetic, and therefore chemical shift changes upon adsorption are straightforward to interpret. The Ru and Fe complexes are comparatively unreactive toward silica surfaces. Only minimal decomposition is expected for 2 and 3,¹² and trace amounts of ferrocenium salts might be formed from 5.¹³ Therefore, ¹H and ¹³C as well as ²H solid-state NMR methods are applied in this contribution to probe a possible increase in mobility when progressing from the crystal lattice to a surface monolayer. Additionally, offering different surface polarities with rigorously dried, hydrophobic silica, and also silica with adsorbed water and silane-modified silica,⁹ should enhance the general knowledge about the characteristics of surface-adsorbed species.

II. RESULTS AND DISCUSSION

The substances 1–5 (Scheme 1) have been adsorbed by grinding the dry components together with silica as described in the Experimental Section to give the adsorbed species 1a–5a. The adsorption process is fast; after grinding the dry components for 1.5 min, 88% of the material is adsorbed within the first 5 min and 95% within the first 2 h. For the following experiments, the amounts have been calculated to give submonolayer coverages, so that the molecules would not be impeded in their movement by overly dense packing on the surface. For 5a, different amounts have been applied (see below).

Assuming that all metallocenes are adsorbed by interaction of the π systems of their Cp ligands with the surface, in analogy to the PAH,^{5,6,10} they should “stand upright” on the surface. Figure 1 shows a to-scale artist’s rendering of a metallocene in an idealized straight pore with a diameter of 40 Å. In principle, the metallocene could also lie on the surface sideways, with the Cp–M–Cp axis aligned parallel to the surface and the Cp ligands functioning like the wheels on a car axle. However, this would imply that the Cp rings are oriented perpendicular to the surface and the interaction of the metallocenes with the surface would take place via the hydrogen atoms of the ligands. This scenario is unlikely, because aromatic compounds such as tetraphenylmethane, whose “prickly” geometry excludes a parallel orientation of the phenyl rings to the surface sterically, cannot be adsorbed on a silica surface.^{8f} Even at higher temperatures or after dissolving the tetraphenylmethane prior to the adsorption on silica to surmount the lattice energy, the molecules do not adsorb.^{8f} While more proof against the static sideways orientation will be given below, it cannot be excluded that the metallocene molecules reorient quickly and isotropically around the metal center in sort of a “tumbleweed”

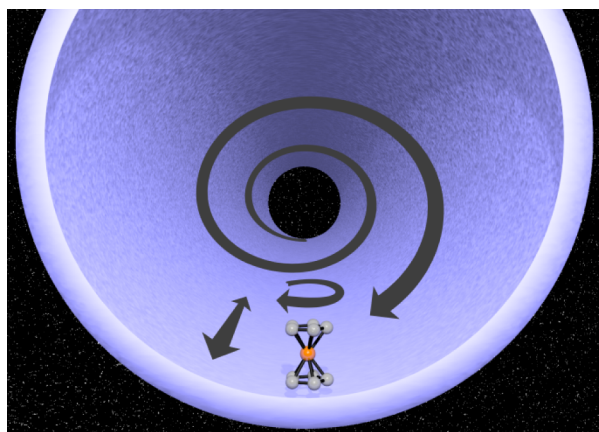


Figure 1. Modes of mobility when a metallocene molecule is adsorbed on the surface within an idealized silica pore.

scenario. This mode of mobility would in principle reduce the residual line widths and CSA of the adsorbate signals. However, taking into account that the interaction of an aromatic system with the surface is strong enough to break down crystal lattices,^{3,5,6} this mode of mobility seems less likely.

Starting at this point, Figure 1 depicts the potential modes of mobility across the surface. Translational mobility back and forth within the pores is essential for forming monolayers of molecules by direct interaction of the polycrystalline materials 1–5 with silica surfaces. There needs to be a “melting process” to overcome the packing forces of the crystal lattice, which also enables the adsorbate molecules to move deeper into the silica pores, making room for additional molecules to adsorb. It is assumed that this mode of mobility continues after consumption of the crystals and formation of the monolayers and does not occur only at the time of the initial contact. This will be corroborated later by probing the mobilities of 5a with different surface coverages. Overcoming the crystal packing forces for 1–5 needs substantial efforts, since their melting points are comparatively high, at 197–200 °C for 1,^{14a} 200–201 °C for 2,^{14b} 66–67 °C for 3,^{14b} 60–61 °C for 4,^{14c} and 169 °C for 5.^{14d}

Since the surface of the pores within amorphous silica is not planar but concave (Figure 1), the adsorbed molecules can travel inside the pores on a spiraling trajectory, which results in isotropic reorientation of the molecules in space. This motion might be responsible for the reduction of the CSA and the residual line widths of the signals of 1a–5a. It has to be noted that basically the whole surface of the mesoporous silica is located inside the pores since the average particle size is very large with diameters of 0.063 to 0.2 mm. One cubic centimeter of the applied silica weighs 0.515 g, and spheres fill approximately 74% of space, so it can be calculated that even for the smallest particle diameter of 0.063 mm only about 2% of the overall surface area of 750 m²/g counts as surface outside of the pores. For the presented application this is negligible, and we therefore assume that basically all molecules are adsorbed on the surface within the pores.

Cp rings in metallocenes rotate even in the crystalline materials;^{4a} therefore we assume this ring rotation also occurs in the adsorbed molecules (Figure 1). Since this mode of mobility is already present in the polycrystalline materials, it is unlikely to contribute to the reduction of the line widths or the CSA of the adsorbed metallocenes in a major way.

When polycrystalline Cp₂Ru (1) is mixed with silica, it is adsorbed on the surface as 1a. Figure 2 shows the drastic

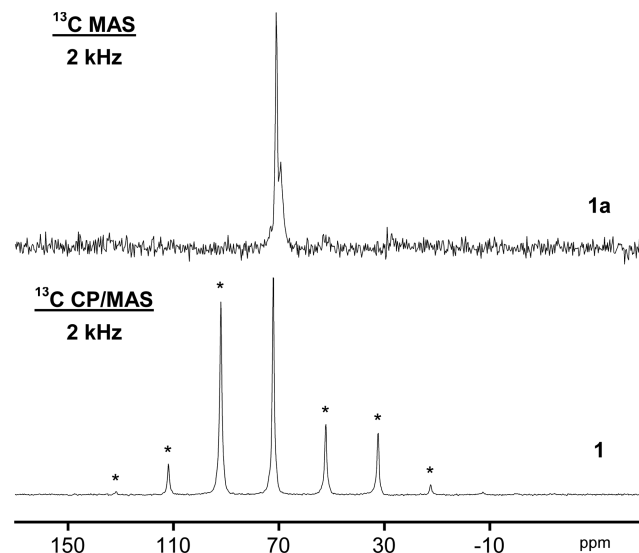


Figure 2. 100.6 MHz ¹³C CP/MAS NMR spectrum of polycrystalline 1 (bottom) and single pulse excitation ¹³C MAS NMR spectrum of adsorbed 1a (top). The asterisks denote rotational sidebands.

change in the ¹³C solid-state NMR spectra of 1 versus 1a. The signal of polycrystalline 1 displays a large CSA, with a span^{4b} of 81.3 ppm, which manifests itself in a multitude of rotational sidebands when the sample is spun and a large wide-line pattern without spinning. The elements of the CSA ($\delta_{\text{iso}} = 72.2$, $\delta_{11} = 99.7$, $\delta_{22} = 98.3$, $\delta_{33} = 18.4$ ppm) have been obtained from the wide-line pattern and by simulation using the spectrum with rotation.¹⁵ While the isotropic chemical shift changes only minimally upon adsorption, from 72.2 to 71.1 ppm, the CSA basically vanishes. A small shoulder at the signal might be attributed to residual polycrystalline material or an impurity not visible in the spectrum measured with cross-polarization. Since the residual line width of the CP/MAS signal of polycrystalline 1 is already very small, with a value of 63 Hz (Figure 2), the change upon adsorption to the resulting line width of 91 Hz for 1a does not seem substantial. It should be mentioned, however, that upon recording the spectrum of 1 with a single pulse program without decoupling, the residual line width amounts to 895 Hz, which means that contemplating this comparison the line width decreases by 804 Hz upon adsorption.

Looking at the ¹H MAS spectra of 1 and 1a (Figure 3), however, besides the obvious reduction of the CSA, the residual line width is reduced substantially from 1.25 kHz for 1 to merely 88 Hz for 1a. The low-intensity background signals at high field in the ¹H MAS spectrum of 1a (Figure 3, top) stem mainly from the protons in silica and are also observed in the spectra of other adsorbed species. When a rotor is filled with silica and a ¹H MAS spectrum is recorded using the same measurement conditions and parameters, including the receiver gain, the small background signal is observed. It can be subtracted from the ¹H MAS spectrum of 1a without distortions of the baseline, yielding a clean spectrum with a symmetric center line (not shown). Again, the isotropic chemical shift changes only minimally on going from 1 with $\delta_{\text{iso}} = 4.6$ ppm to 1a with 4.5 ppm. So, overall, Cp₂Ru behaves very similar to Cp₂Cr and Cp₂Fe with respect to adsorption and the ensuing changes in the solid-state NMR spectra.³

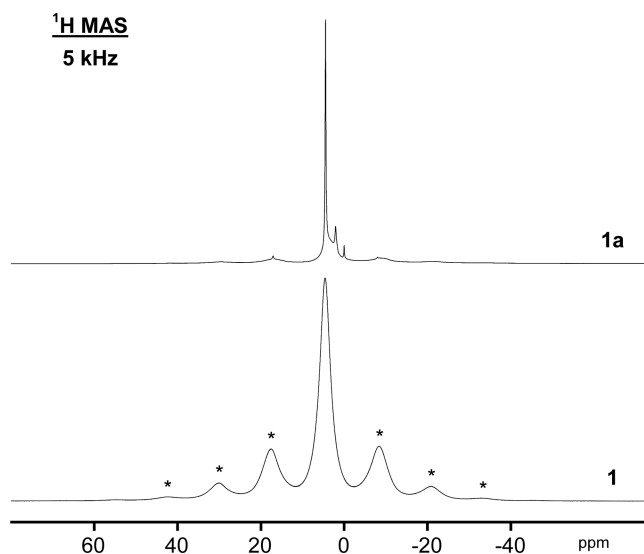


Figure 3. Single-pulse excitation 400.1 MHz ^1H MAS NMR spectra of polycrystalline **1** (bottom) and adsorbed **1a** (top). Asterisks denote rotational sidebands.

Next, in order to test whether an extended aromatic system in the ligand would change the adsorption potential of a metallocene, $(\text{Ind})_2\text{Ru}$ (**2**) (Scheme 1) has been adsorbed in a submonolayer on silica. The ^{13}C CP/MAS spectra are shown in Figure 4. At a spinning speed of 11 kHz the signals of

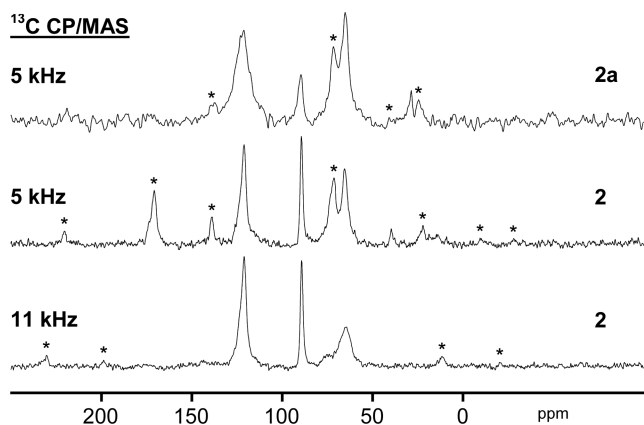


Figure 4. 100.6 MHz ^{13}C CP/MAS NMR spectra of polycrystalline **2** (bottom: 11 kHz, middle: 5 kHz rotational frequency) and adsorbed **2a** (top, 5 kHz). Asterisks denote rotational sidebands.

polycrystalline **2** have only small first-order rotational sidebands left. Therefore, the comparison between **2** and **2a** is based on 5 kHz measurements, where second-order rotational sidebands are visible for **2**. Most relevant diagnostically is the signal of the olefin carbon nuclei at 121.1 ppm¹⁶ with their intrinsically large CSA.^{4b} Again, upon adsorption, the number and intensity of the rotational sidebands are greatly diminished, which is best seen by the disappearance of the large sideband at 170.8 ppm of the olefin carbon resonance. While there is no doubt that adsorption of **1** to form **1a** takes place, due to the reduced CSA, the extended π system of the indenyl ligands makes a difference. The residual line width is increased from 297 Hz for **2** to 358 Hz for **2a**. This effect might indicate that the molecules are more strongly adsorbed and therefore less mobile on the surface. Alternatively, one could speculate that with the

extended ligands potential “tumbleweed” or rolling sideways modes of mobility might be inhibited, in this way leading to adsorbed, but less mobile surface species. It would also be plausible that the larger ligands inhibit the mobility on the nonplanar surface in the pores of the amorphous silica. However, the increased residual line widths for **2a** could also stem from a slight decomposition of **2** on the surface,¹² creating Ru nanoparticles. This would also account for the relatively poor S/N ratio (Figure 4).^{4c}

In order to test this hypothesis, we sought to employ a metallocene with the same center metal Ru and an extended ring system of about equal dimensions, but without a conjugated aromatic system. Bis(tetrahydroindenyl)ruthenium (**3**, Scheme 1) offered itself as a logical choice. The proton NMR data of complex **3** have been given in the literature,¹⁷ and we added the ^{13}C chemical shifts and assigned the signals by an HSQC measurement. Surprisingly, in contrast to the single-crystal X-ray data available for **2**,¹⁸ none are in the literature for **3**. Figure 5 shows the obtained single-crystal X-ray structure of

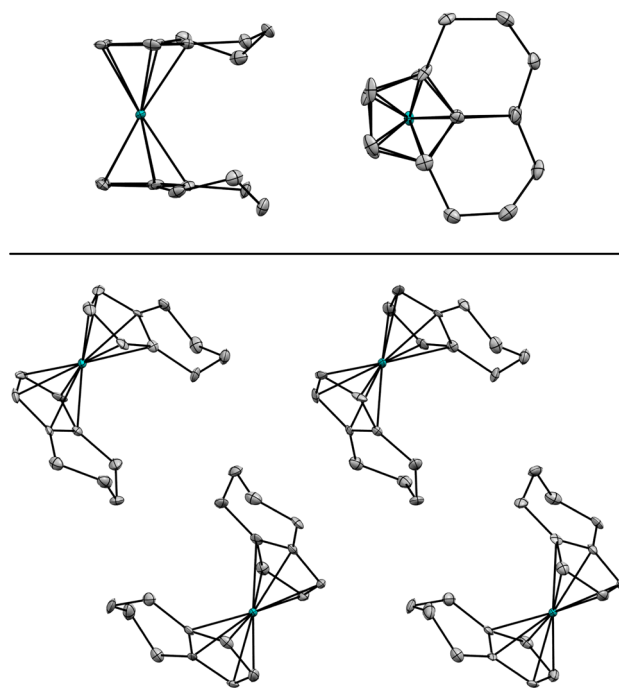


Figure 5. Single-crystal X-ray structure of **3**.¹⁹ Packing of the molecules in the unit cell (bottom) and side (top left) and top view (top right) of one molecule. Thermal ellipsoids are shown at the 50% probability level. Hydrogen atoms are omitted for clarity.

3.¹⁹ Interestingly, the Cp moieties of the ligands are not stacked on top of each other, a pattern that unsubstituted metallocenes often assume. Although not quite intercalated due to steric constraints, the aliphatic substituents are seeking close proximity to each other. The top view (Figure 5, top right) shows that the aliphatic rings are eclipsed with a torsion angle of about 67.1° . The side view (Figure 5, top left) reveals a substantial deviation of the ligands from planarity. The aliphatic carbons and protons deviate from the plane of the Cp ring by as much as 0.50 and 1.47 Å. Therefore, by studying the adsorption characteristics of **3**, the effect of slight nonplanarity of the ligands can be observed as well.

There are four molecules in the unit cell of **3**, with two sets of magnetically inequivalent ^{13}C nuclei (Figure 5, bottom).¹⁹

Therefore, a double signal set is expected in the ^{13}C CP/MAS spectrum of polycrystalline **3**. The bottom spectrum of Figure 6

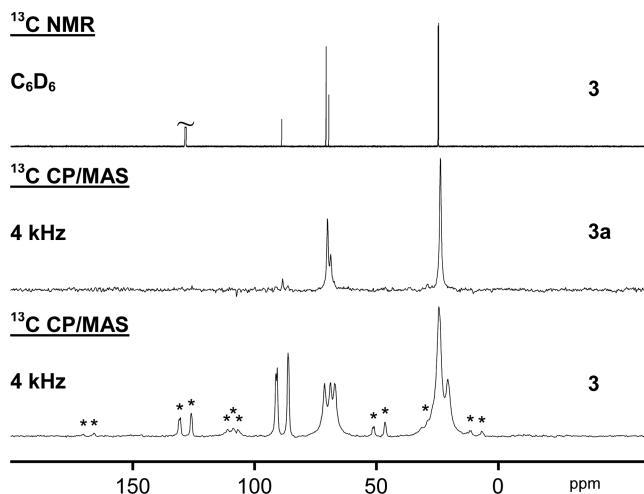


Figure 6. 100.6 MHz ^{13}C CP/MAS NMR spectra of polycrystalline **3** and adsorbed **3a** (bottom two spectra) and **3** dissolved in benzene- d_6 (top). Asterisks denote rotational sidebands.

shows that this is indeed the case. As expected the signals of the aliphatic ^{13}C nuclei at 20.5 and 24.4 ppm have only minimal CSA,^{4b} which can be deduced from the absence of rotational sidebands at a spinning speed of only 4 kHz. The resonances of the Cp ring carbon nuclei in the regions of the CH signals at 67.1, 69.0, and 71.4 ppm and the quaternary C signals at 86.3, 90.8, and 91.4 ppm, however, display the elaborate sets of rotational sidebands similar to those of **1** and **2**. Upon adsorption, the appearance of the ^{13}C CP/MAS spectrum is thoroughly changed (Figure 6, middle). The average line width in the spectra decreases from 85 Hz for **3** to 49 Hz for **3a**, and all rotational sidebands are gone. For comparison, the spectrum of **3**, dissolved in benzene- d_6 , is added as the top trace in Figure 6. This result shows not only that **3** is adsorbed on a silica surface but that, in contrast to anticipation, the cyclic alkyl substituent even seems to facilitate the mobility of the molecules of **3a** across the surface. In fact, the properties of **3a** are more similar to those of dissolved **3** than to polycrystalline **3**. Furthermore, this result rules out that the increased space requirement of the indenyl ligand in **2** is responsible for the comparatively broad residual lines of **2a**. Finally, one can assume that a tumbleweed mobility or rolling of **3a** via the ligands on the surface is extremely unlikely, as it is hard to imagine that these processes would not be impeded by the bulky alkyl substituents. We conclude that the extended aryl systems of the ligands in **2a** lead to strong adsorption and that alkyl substituents instead of a conjugated ring system enhance the mobility of **3a** across the silica surface.

Next, we sought to elucidate the effect of the alkyl substituents in **3** by probing the adsorption of an alkane on silica. Cyclododecane (**4**, Scheme 1) emerged as a viable candidate due to its comparatively high melting point (see above) and known solid-state NMR characteristics.²⁰ Surprisingly, **4** adsorbs readily on silica to give **4a**, which can be seen in the narrower residual line width of the ^{13}C CP/MAS signals (Figure 7) of **4a** (18 Hz) as compared to **4** (60 Hz). However, even at the low spinning speed of 2 kHz there are no rotational sidebands for the signal of **4**, indicating the low starting CSA of

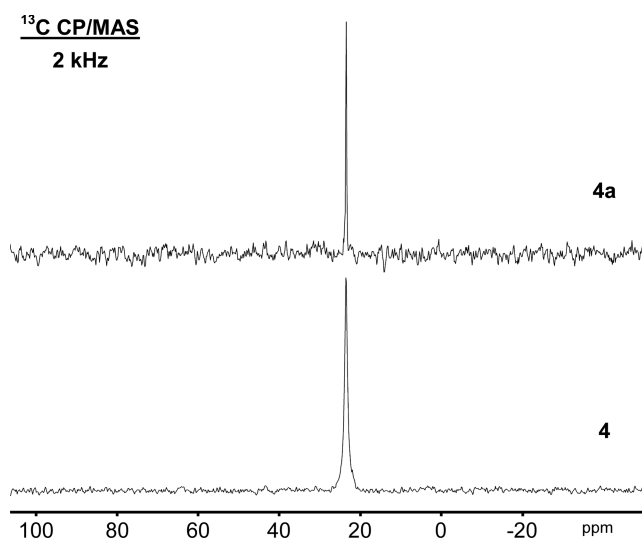


Figure 7. 100.6 MHz ^{13}C CP/MAS NMR spectra of polycrystalline **4** and adsorbed **4a**.

alkanes.^{4b} Furthermore, the $\delta(^{13}\text{C})$ changes only minimally from 23.64 ppm for **4** to 23.63 for **4a**.

Therefore, the ^1H MAS spectra of **4** and **4a** are diagnostically more valuable, because the large dipolar interactions guarantee multiple sets of rotational sidebands (Figure 8, bottom) for the

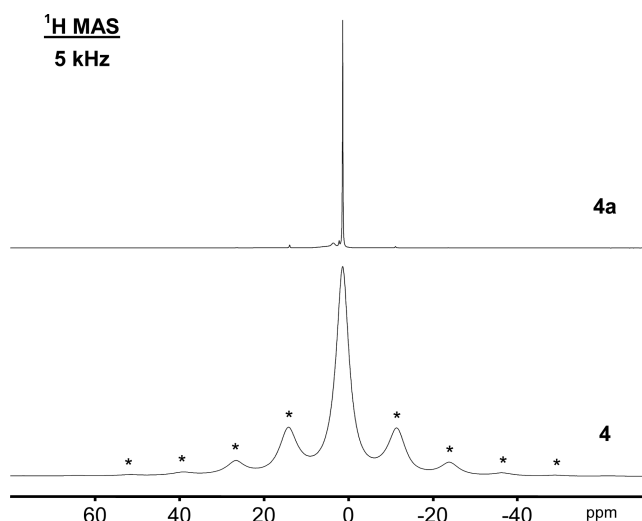


Figure 8. 400.1 MHz ^1H MAS NMR spectra of polycrystalline **4** (bottom) and adsorbed **4a** (top). Asterisks denote rotational sidebands.

pure material, which vanish upon adsorption due to the increased mobility on the surface (Figure 8, top). The $\delta(^1\text{H})$ on the other hand changes minimally from 1.42 ppm for **4** to 1.39 ppm for **4a**.

Since the melting point of dodecane is below 100 °C (see above), one could argue that the adsorption on silica might be facilitated by the pressure exerted on the sample during spinning and the slightly raised temperature within the rotor at a rotational speed of 5 kHz.^{2b} Therefore, the ^1H solid-state NMR spectra have also been recorded without sample spinning, a technique that earlier yielded crucial results in adsorption studies³ and in polymer chemistry.²¹ Indeed, even in the absence of elevated temperatures and pressures the largest

effect of adsorbing **4** can be seen in the ^1H wide-line NMR spectra of **4** as compared to **4a** (Figure 9). The line width

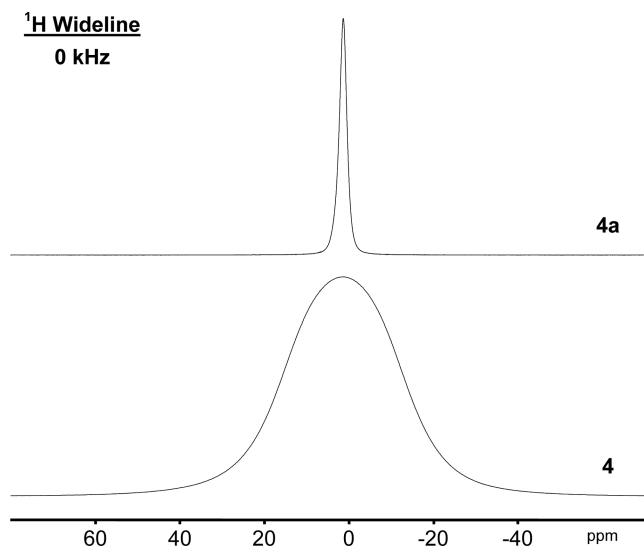


Figure 9. 400.1 MHz ^1H wide-line NMR spectra of polycrystalline **4** and adsorbed **4a**.

changes from 12.2 kHz for **4** to only 810 Hz for **4a**. The ^1H chemical shifts again undergo only minimal change from 1.4 ppm for **4** to 1.3 ppm for **4a**. The fact that cyclododecane is adsorbed so readily demonstrates impressively that van der Waals interactions can be responsible for breaking up crystal lattices, leading to the adsorption of alkanes. This phenomenon might be interesting for applications in the oil and gas industry.²²

Next, the quest for a more quantitative insight into the mobility of surface-adsorbed species inspired us to study the phenomenon by ^2H solid-state NMR spectroscopy. It is known that ^2H NMR in the solid state yields information on mobilities via the quadrupolar coupling constant Q_{CC} , which can be derived from the splitting of the most intense lines in the Pake patterns.^{4a} The correlation between reorientation times and appearances of the corresponding Pake patterns has been described in detail.²³ More recently, ^2H solid-state NMR has also been applied to obtain more quantitative insight into various other dynamic scenarios.²⁴ For example, the segmental dynamics of polymer chains^{24b,c} and a plasticization of poly(vinyl acetate) adsorbed on silica have been investigated.^{24a} One of us has shown earlier that a ^2H MAS Pake pattern of fully deuterated polycrystalline chromocene can be measured,^{2b} although the compound is paramagnetic. Therefore, we synthesized deuterated ferrocene **5** (Scheme 1) according to the literature method²⁵ from the robust and inexpensive Cp_2Fe .

When polycrystalline **5** is measured without sample spinning, the typical Pake pattern results.^{4a} The splitting of the most intense lines of the Pake pattern is 72.5 kHz, which is in agreement with the literature.²⁶ The ^2H MAS spectrum of polycrystalline **5** is shown at the bottom of Figure 10. The splitting of the most intense lines, as well as the quadrupolar coupling constant of 96.9 kHz, as defined by ref 4a, can also be obtained from this spectrum using a line-fitting routine.¹⁵ When **5** is applied to silica in a submonolayer quantity of 120 mg per g of SiO_2 (Figure 10, top), the Pake pattern collapses and a narrow line with a half-width of merely 170 Hz arises. Together with the absence of any rotational sidebands this

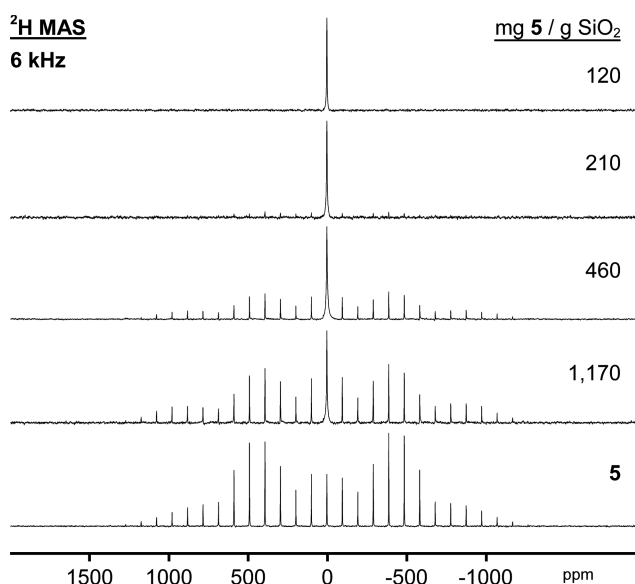


Figure 10. 61.4 MHz ^2H MAS NMR spectra of polycrystalline **5** (bottom) and **5a** adsorbed on silica with the indicated wt % amounts.

indicates that **5** is completely adsorbed to form **5a** and that the molecules must experience isotropic mobility across the surface. A comparison with typical ^2H solid-state NMR lineshapes given in the literature²³ indicates that the reorientation time should be shorter than 1 ns.

When increasing amounts of **5** are applied to silica, as indicated in the ^2H MAS spectra of Figure 10, besides the narrow peak of adsorbed **5a** the Pake pattern of the residual polycrystalline material **5** is growing in intensity. Importantly, the transition from the adsorbed to the polycrystalline state is abrupt. There is no gradual increase of the signal line width of **5a**, which would indicate the formation of multilayers on the surface. Therefore, we conclude that there is no stacking of the molecules of **5a** on the surface, as it could be assumed from the packing of Cp_2Fe in the single crystal.²⁷

The ^2H MAS spectra obtained after applying different amounts of **5** to silica allow the quantitative determination of adsorbed versus leftover polycrystalline material. With this ratio of **5a**:**5** the maximal surface coverage with molecules of **5a** in a monolayer can be obtained. The only complication in evaluating the spectra such as the ones shown in Figure 10 is that the ^2H chemical shift does not change substantially when going from **5** with 4.37 ppm to **5a** with 4.43 ppm. Therefore, the isotropic lines are overlapping, as displayed in Figure 11, and need to be subjected to deconvolution.²⁸ The rotational sidebands and the narrow central line with half-widths of only 41 Hz belong to the Pake pattern of the polycrystalline material **5**, while the single broader component of the central line belongs to adsorbed **5a**.

Figure 11 demonstrates that the deconvolution process²⁸ leads to an excellent fit of the sum of the deconvoluted signals with the experimental spectrum. When determining the ratio of **5a**:**5**, one needs to take care to add the intensities of all rotational sidebands of the Pake pattern to the intensity of the central line of **5**. When a large excess of **5** is applied to the silica, the maximal surface coverage of 118 molecules of **5a** per 100 nm^2 of silica surface can be determined from the ratio of adsorbed to polycrystalline material after deconvolution. Figure 12 depicts the view on a silica surface with maximal surface coverage. The footprint of **5a**, standing upright on the surface,

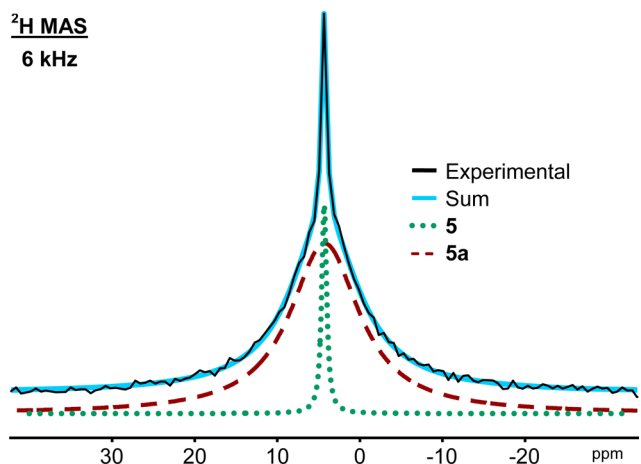


Figure 11. Deconvolution²⁸ of the overlapping isotropic lines of the ^2H MAS signals of residual polycrystalline **5** (narrow line) and adsorbed **5a** (broad signal) after grinding 460 mg of polycrystalline **5** with 1 g of silica (Figure 10, third trace).

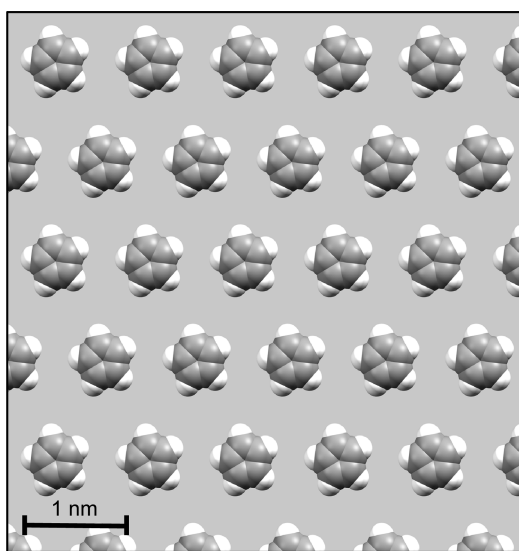


Figure 12. To-scale image depicting the maximum surface coverage of 118 molecules of adsorbed **5a** on 100 nm^2 of silica that was obtained after grinding **5** with silica; 25 nm^2 of the surface is shown.

was calculated based on the distance between the center of the Cp ring and an H atom (2.302 Å) and taking the van der Waals radius of H into account to give an overall radius of 3.502 Å. Assuming hexagonal packing of these circles on the surface, about 201 $\text{Cp}_2\text{Fe-d}_2$ molecules can maximally occupy 100 nm^2 of surface area in a monolayer, corresponding to 2.50 mmol of **5** adsorbed per g of silica.

Interestingly, comparing the calculated maximal density of **5a** (201 molecules per 100 nm^2) with the experimental value (118 molecules, Figure 12), there seems to be ample free “wobble space” left between the ferrocene molecules. This is another indication that not only ring rotation but also translational mobility has to happen on the surface. With a theoretically densest packing on the surface there would not be enough room left for this translational movement, and therefore the “melting” of the crystal onto the silica surface could not happen.

The number of adsorbed molecules of **5a** depends on the amount of applied polycrystalline **5**. The graphical display in

Figure 13 shows that the more **5** is applied, the denser the packing of the surface with **5a** becomes in the case of the well-

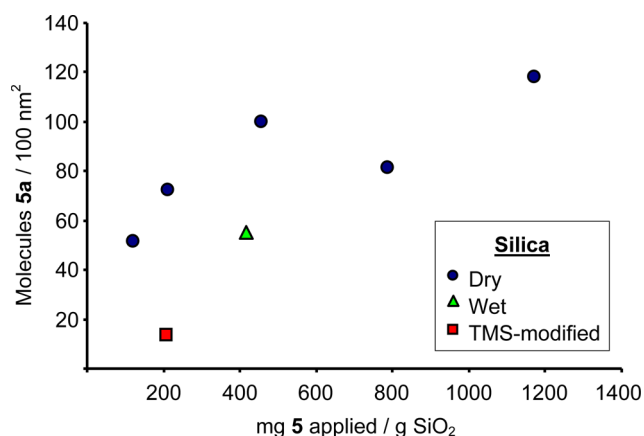


Figure 13. Amount of **5a** adsorbed on silica after its treatment with different amounts of **5**.

dried silica. Since it is known that the nature of the surface also acts as a major factor determining surface coverages,²⁹ wet silica (see Experimental Section), with a hydrophilic surface and maximal number of silanol groups, and the hydrophobic trimethylsilyl (TMS)-modified silica,⁹ where the silanol protons are removed by end-capping, have also been tested with respect to the surface coverage. As Figure 13 shows, the surface coverage of **5a** on 100 nm^2 of wet silica is much lower than in the case of well-dried support, when applying a similar amount of **5**. Since **5** is not hydrophilic in nature and should in principle be attracted to TMS-modified silica by van der Waals interactions, this result shows that surface silanol groups are mainly responsible for the adsorption of **5a**. In the case of an excess of water on the surface, however, **5** might be repelled by the water layer on the surface due to its hydrophobic nature, and therefore the surface water layer prohibits interactions with the surface silanol groups underneath.

Although the TMS-modified silica is hydrophobic like the silica dried rigorously at high temperature in vacuo, the adsorption of **5** is minimal, with only 13 molecules of **5a** on 100 nm^2 of the modified silica. In comparison, using the same amount of **5** on well-dried silica, 72 molecules of **5a** are found on the surface. Again, the missing interaction with surface silanol groups might prevent the formation of large amounts of **5a**. Additionally, the TMS groups might act as mechanical obstacles for the translational mobility of **5a**, inhibiting the “flow” of ferrocene molecules from the crystal onto the surface.

The assumptions that the $(\text{CH}_3)_3\text{Si}$ groups on the surface form an obstacle for the adsorbed molecules of **5a** and that surface silanol protons are advantageous for adsorption are also reflected in the comparatively large line width at the low surface coverage of 13 molecules on 100 nm^2 of surface area (Figure 14). In contrast to the situation with wet silica, in the case of dry silica as the support a correlation between the line width and the surface coverage can be found, as indicated by the fitting line in the graph of Figure 14. The higher the surface coverages, the larger the residual line widths of the ^2H MAS signals of **5a** become. This again speaks for the assumption that less free space on the surface impedes the mobility of the molecules.

Encouraged by the narrow solid-state NMR lines obtained for the adsorbed species **1a–5a**, we wondered whether the fast

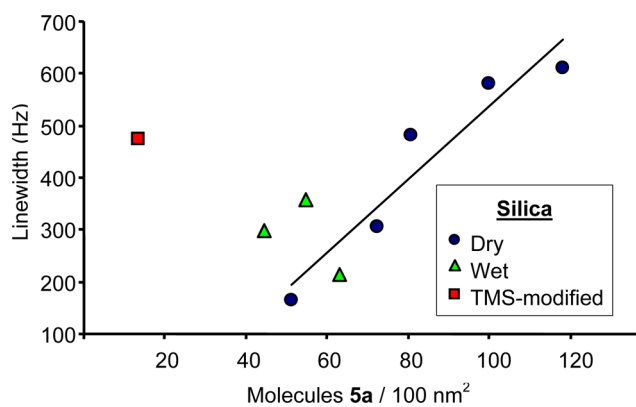


Figure 14. Residual line widths of the ^2H MAS signal of **5a** adsorbed on silica after its treatment with different amounts depending on its surface coverage on silica.

isotropic reorientation of the molecules would approach the mobility of the molecules in solution. Therefore, we tested whether ^1H and ^{13}C NMR signals would also be visible when filling a powder of silica with surface-adsorbed Cp_2Fe into a conventional 5 mm glass NMR tube to a height of 3 cm each and measuring this sample on a liquids NMR instrument. As a comparison, polycrystalline Cp_2Fe has been ground finely and also filled into a 5 mm sample tube. Interestingly, both ^1H and ^{13}C NMR signals of adsorbed Cp_2Fe emerge with high S/N ratio after only 32 and 128 scans, respectively. The ^{13}C NMR spectrum of adsorbed Cp_2Fe is shown at the top of Figure 15.

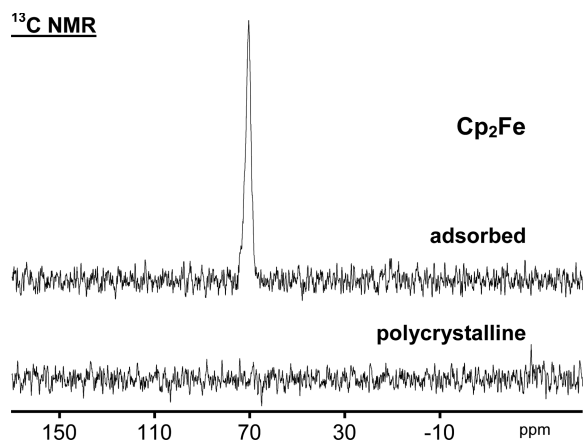


Figure 15. 125.7 MHz $^{13}\text{C}\{^1\text{H}\}$ NMR spectra of polycrystalline (bottom) and adsorbed (top) Cp_2Fe , recorded on a standard liquids NMR spectrometer.

Being able to observe a narrow signal with a liquids NMR instrument without high-power capabilities means that the mobilities of the Cp_2Fe molecules across the surface are indeed fast and isotropic and that they come close to the mobilities of the molecules dissolved in liquids. The ^1H NMR of a polycrystalline Cp_2Fe sample has a line width of 23.6 kHz, and there is an obvious background signal of the glass of the sample tube and the probehead visible. The sample of adsorbed Cp_2Fe , however, exhibits a narrow signal of only 1.1 kHz in the ^1H NMR spectrum, and the background signal is broad and of negligible intensity. The difference between adsorbed and polycrystalline Cp_2Fe is even more pronounced when comparing their ^{13}C NMR spectra (Figure 15). While the

polycrystalline Cp_2Fe gives, as expected, no signal due to the chemical shift anisotropy and large heteronuclear dipolar interactions, the adsorbed ferrocene results in a narrow signal with a half-width of only 251 Hz because all anisotropic interactions are diminished substantially by the mobility of the adsorbed species. Therefore, we conclude that it is possible to record spectra of metallocenes adsorbed on silica surfaces even with conventional liquids NMR spectrometers due to the nearly isotropic fast motion of the adsorbed molecules across the surface as described for Figure 1.

In order to probe qualitatively the strength of adsorption and make the “melting” of the crystals onto the silica surface more plausible, the following experiment has been performed: Cp_2Fe and Cp_2Fe adsorbed on silica have been subjected to sublimation under the same vacuum. As expected, polycrystalline Cp_2Fe sublimed already at 55 °C, growing into large crystals. In principle, the adsorbed Cp_2Fe could profit from the advantage of being prearranged in a monolayer, allowing for a quick and simultaneous detachment of all molecules from the surface. However, no trace of sublimed ferrocene forms from the silica-adsorbed material, even after prolonged time to make up for any pore diffusion requirement. Only upon heating to about 73 °C does the adsorbed metallocene sublime. This result again confirms that the attraction of Cp_2Fe to the surface is stronger than the forces keeping the single crystals packed. A more quantitative study is sought in future work.

III. CONCLUSION

It has been demonstrated unequivocally by ^1H and ^{13}C solid-state NMR techniques that all metallocenes **1–3** and **5**, as well as dodecane, are readily adsorbed on a silica surface even in the absence of a solvent after dry grinding at ambient temperature and that they undergo translational mobility. The influence of an extended π system, as in **2**, on the adsorption, as well as the impact of hydrophobic substituents with large steric demand, as realized in **3**, have been probed. Additionally, it has been demonstrated that an alkane with a high melting point (**4**) can be adsorbed on a silica surface. Different modes of mobility are discussed, and a timeline for isotropic reorientation has been established by ^2H MAS NMR of adsorbed **5a**. No indication for stacking of the metallocene molecules on the surface has been found, as the transition from polycrystalline state to an adsorbed monolayer is abrupt. A correlation between the surface coverage and the mobility of the adsorbed molecules has been described. Wet and TMS-end-capped silica as supports lead to smaller amounts of adsorbed material and, in the latter case, lower surface coverage and broader lines. Finally it is demonstrated in the case of Cp_2Fe that the surface-adsorbed species can be measured using a conventional liquids NMR spectrometer because of the short reorientation time that diminishes anisotropic interactions substantially. In future studies the modes of mobility will be defined and their extents quantified for **1a–5a**. The ^{13}C T_1 and ^1H T_2 relaxation times,²¹ as well as CSA values will be measured at different temperatures. The reversibility of the adsorption process, as well as the variation of the maximal surface coverage with temperature, will be tested by VT NMR measurements.

IV. EXPERIMENTAL SECTION

The ^1H , ^{13}C , and HSQC measurements of liquids and of silica-adsorbed and polycrystalline ferrocene (Figure 15) were performed on a Varian 500 MHz liquids NMR spectrometer. The ^1H , ^2H , and ^{13}C solid-state NMR spectra were recorded with a Bruker Avance 400

wide-bore spectrometer using a 4 mm MAS probehead. All samples were measured by packing the whole rotors with finely ground polycrystalline material or filling the silica in loosely. Compressed air was used as both the bearing and drive gas for the MAS measurements. The recycle delays were 3 s for the ^{13}C CP/MAS and 10 s for the single-pulse NMR measurements, and 3 s for recording the ^1H and ^2H NMR spectra. For the ^{13}C MAS measurements ^1H high-power decoupling was turned off or applied as detailed in the text. Typically 64 transients were accumulated for ^1H and 2400 for ^{13}C solid-state NMR measurements, with the exception of **2a** and **3a**, which needed ca. 26 000 scans. The spectra of polycrystalline and adsorbed Cp_2Fe were obtained on a Varian 500 liquids NMR instrument with Waltz decoupling and a pulse delay of 2 s, and 16 and 128 transients were collected for the ^1H and ^{13}C measurements. The ^{13}C NMR signal was referenced relative to benzene in a capillary (128.00 ppm) to give a chemical shift of 70.38 ppm for the resonance of the adsorbed Cp_2Fe .

For obtaining the adsorbed species **1a–5a** and adsorbed Cp_2Fe , the polycrystalline materials have been ground together with the corresponding type and amount of silica by hand for 1.5 min using a mortar and pestle. For **1** and **2** this process was carried out in the glovebox; in all other cases the grinding step was performed on the benchtop. The following values give the amounts with respect to 1 g of support: **1** (268.8 mg, 1.162 mmol), **2** (243.0 mg, 0.733 mmol), **3** (244.1 mg, 0.719 mmol), and **4** (178.7 mg, 1.062 mmol). For **5**, the different amounts are given in Figure 13. For this measurement series of **5a** the dry mixtures of were allowed to stand for at least 2 h prior to the measurements. For recording the ^1H and ^{13}C NMR spectra on the liquids NMR spectrometer (Figure 15) an amount corresponding to 488.7 mg (2.627 mmol) per g of silica has been applied.

Deconvolution and processing of the spectra was accomplished using ACD/NMR Processor Academic Edition.²⁸ The quadrupolar coupling constants were derived from the ^2H MAS NMR spectra using the NMR simulation program Dmfit.¹⁵ The best fit line in Figure 13 was obtained using only the data derived from the dry SiO_2 , and the R^2 value was 0.905, which indicates a strong correlation.

Conventional silica gel, as used, for example, for column chromatography has been purchased from Merck. Its average pore diameter is 40 Å, the average particle size is 0.063–0.2 mm, and the specific surface area 750 m^2/g . The silica gel was either dried in vacuo at 250 °C for 40 h (referred to as dry SiO_2) or used as received (wet SiO_2). The Me_3Si -modified silica was prepared as described previously.⁹

Compounds **1** and **4** were purchased from Strem Chemicals and TCI America, respectively. The crystalline complexes **2** and **3** were used as received from Dr. K. Öfele, TU Munich. While the ^{13}C NMR signal assignments are known for **2**,¹⁶ we obtained the NMR signal assignments for **3** using a 2D HSQC NMR spectrum and the ^1H signal assignments given in the literature.¹⁷ $\delta(^{13}\text{C})$ (125.66 MHz, C_6D_6 [ppm]): 88.52 (C_q), 70.34 (CHC_q), 69.19 (CHCHC_q), 24.33 ($\text{C}_q\text{CH}_2\text{CH}_2$), 24.12 (C_qCH_2). Compound **5** was obtained by preparing 1,1'-dilithioferrocene according to a literature method²⁵ and subsequent quenching with D_2O .

■ ASSOCIATED CONTENT

■ Supporting Information

The CIF file of the single-crystal X-ray structure determination of **3**. This material is available free of charge via the Internet at <http://pubs.acs.org>.

■ AUTHOR INFORMATION

■ Corresponding Author

*Fax: (+1)-979-845-5629. Phone: (+1)-979-845-7749. E-mail: bluemel@tamu.edu.

■ Notes

The authors declare no competing financial interest.

■ ACKNOWLEDGMENTS

This material is based upon work supported by The Welch Foundation (A-1706), the National Science Foundation (CHE-0911207, CHE-0840464, and CHE-1300208), and the APPEAL Consortium. We thank Darcie Hicks for doing some experiments. Furthermore, we thank Dr. K. Öfele (TU Munich) for samples of **2** and **3**.

■ REFERENCES

- (1) Rebenstorf, B.; Panda, C. J. *Mol. Catal.* **1991**, *65*, 173–180.
- (2) (a) Schnellbach, M.; Blümel, J.; Köhler, F. H. *J. Organomet. Chem.* **1996**, *520*, 227–230. (b) Blümel, J.; Herker, M.; Hiller, W.; Köhler, F. H. *Organometallics* **1996**, *15*, 3474–3476.
- (3) Cluff, K. J.; Schnellbach, M.; Hilliard, C. R.; Blümel, J. *J. Organomet. Chem.* **2013**, *744*, 119–124.
- (4) (a) Fyfe, C. A. *Solid-State NMR for Chemists*; C.F.C. Press: Guelph, Canada, 1983. (b) Duncan, T. M. *A Compilation of Chemical Shift Anisotropies*; Farragut Press: Chicago, IL, 1990. (c) Bell, A. T. *NMR Techniques in Catalysis*; Taylor & Francis, 1994. (d) Reinhard, S.; Blümel, J. *Magn. Reson. Chem.* **2003**, *41*, 406–416. (e) Guenther, J.; Reibenspies, J.; Blümel, J. *Adv. Synth. Catal.* **2011**, *353*, 443–460.
- (5) Ebener, M.; Von Fircks, G.; Günther, H. *Helv. Chim. Acta* **1991**, *74*, 1296–1304.
- (6) Günther, H.; Oepen, S.; Ebener, M.; Francke, V. *Magn. Reson. Chem.* **1999**, *37*, S142–S146.
- (7) (a) Baltusis, L.; Frye, J. S.; Maciel, G. E. *J. Am. Chem. Soc.* **1986**, *108*, 7119–7120. (b) Chen, W.-H.; Bauer, F.; Bilz, E.; Freyer, A.; Huang, S.-J.; Lai, C.-S.; Liu, S.-B. *Stud. Surf. Sci. Catal.* **2004**, *154C*, 2269–2274. (c) Grigoriev, D. O.; Senkel, O.; Kretzschmar, G.; Li, J. B.; Noskov, B. A.; Miller, R. *Colloids Surf., A* **1999**, *149*, 81–88.
- (8) (a) Sheng, T.-C.; Kirszenstejn, P.; Bell, T. N.; Gay, I. D. *Catal. Lett.* **1994**, *23*, 119–126. (b) Baltusis, L.; Frye, J. S.; Maciel, G. E. *J. Am. Chem. Soc.* **1987**, *109*, 40–46. (c) Peng, L.; Chupas, P. J.; Grey, C. P. *J. Am. Chem. Soc.* **2004**, *126*, 12254–12255. (d) Sheng, T.; Gay, I. D. *J. Catal.* **1994**, *145*, 10–15. (e) Gay, I. D.; Hu, B.; Sheng, T.-C. *Langmuir* **1999**, *15*, 6132–6134. (f) Yang, Y. *Phosphines and Their Metal Complexes, Adsorbed and Bound by Ionic Interactions on Oxide Supports: A Solid-State NMR Study*. Doctoral dissertation; University of Heidelberg, Germany, 2007.
- (9) Blümel, J. *J. Am. Chem. Soc.* **1995**, *117*, 2112–2113.
- (10) (a) Fyfe, C. A.; Brouwer, D. H. *Can. J. Chem.* **2006**, *84*, 345–355. (b) Fyfe, C. A.; Lee, J. S. *J. Phys. Chem. C* **2008**, *112*, 500–513. (c) Lechert, H.; Basler, W. D. *J. Phys. Chem. Solids* **1989**, *50*, 497–521. (d) Bjarneson, D. W.; Petersen, N. O. *Langmuir* **1991**, *7*, 2821–2826.
- (11) Minakata, S.; Tsuruoka, R.; Komatsu, M. *J. Am. Chem. Soc.* **2008**, *130*, 1536–1537.
- (12) Osiecki, J. H.; Hoffman, C. J.; Hollis, D. P. *J. Organomet. Chem.* **1965**, *3*, 107–112.
- (13) Sato, H. *Hyperfine Interact.* **1990**, *57*, 2089–2094.
- (14) (a) Mercier, A.; Yeo, W. C.; Chou, J.; Chaudhuri, P. D.; Bernardinelli, G.; Kundig, E. P. *Chem. Commun.* **2009**, 5227–5229. (b) Osiecki, J. H.; Hoffman, C. J.; Hollis, D. P. *J. Organomet. Chem.* **1965**, *3*, 107–112. (c) Ruzicka, L.; Stoll, M.; Huyser, H. W.; Boekenoogen, H. A. *Helv. Chim. Acta* **1930**, *13*, 1152–1185. (d) Our own measurement.
- (15) Massiot, D.; Fayon, F.; Capron, M.; King, I.; Le, C. S.; Alonso, B.; Durand, J.-O.; Bujoli, B.; Gan, Z.; Hoatson, G. *Magn. Reson. Chem.* **2002**, *40*, 70–76.
- (16) Kudinov, A. R.; Petrovskii, P. V.; Struchkov, Y. T.; Yanovskii, A. I.; Rybinskaya, M. I. *J. Organomet. Chem.* **1991**, *421*, 91–115.
- (17) Osiecki, J. H.; Hoffman, C. J.; Hollis, D. P. *J. Organomet. Chem.* **1965**, *3*, 107–112.
- (18) Webb, N. C.; Marsh, R. E. *Acta Crystallogr.* **1967**, *22*, 382–387.
- (19) X-ray data for complex **3**: $\text{C}_{18}\text{H}_{22}\text{Ru}$, $M = 339.42$, colorless block, $0.10 \times 0.08 \times 0.04 \text{ mm}^3$, monoclinic, space group Pc (No. 14), $a = 12.3717(14)$, $b = 6.5709(7)$, $c = 17.5678(19)$ Å, $\beta = 96.262(6)^\circ$, $V = 1419.6(3)$ Å³, $Z = 4$, $D_c = 1.588 \text{ g/cm}^3$, $F_{000} = 696$, Bruker GADDS X-ray (three-circle) diffractometer, $K\alpha$ radiation, $\lambda = 1.5418$ Å, $T =$

110(2) K, $2\theta_{\max} = 61.056^\circ$, 29166 reflections collected, 4278 unique ($R_{\text{int}} = 0.0544$). Final GooF = 1.120, $R_1 = 0.0209$, $wR_2 = 0.0514$, R indices based on 4260 reflections with $I > 2\sigma(I)$ (refinement on F^2), 345 parameters, 2 restraints. L_p and absorption corrections applied, $\mu = 8.77 \text{ mm}^{-1}$. Further crystallographic data for this structure have been deposited with the Cambridge Crystallographic Data Center as supplementary publication no. CCDC 989338.

(20) Drotloff, H.; Koegler, G.; Oelfin, D.; Moeller, M. In *Conformationally Disordered Mesomorphic Phases of Cyclododecane and Cyclotetradecane*; Elsevier, 1988; pp 154–158.

(21) (a) Guenther, J.; Wong, M. H.; Sue, H. J.; Bremner, T.; Blümel, J. *J. Appl. Polym. Sci.* **2013**, *128*, 4395–4404. (b) Pope, J.; Sue, H.-J.; Bremner, T.; Blümel, J. *Macromolecules* **2014** in press.

(22) Zheng, Q.; Cai, Z.; Gong, S. *J. Mater. Chem. A* **2014**, *2*, 3110–3118.

(23) Xiong, J.; Lock, H.; Chuang, I. S.; Keeler, C.; Maciel, G. E. *Environ. Sci. Technol.* **1999**, *33*, 2224–2233.

(24) Selected examples: (a) Nambiar, R. R.; Blum, F. D. *Macromolecules* **2009**, *42*, 8998–9007. (b) Hetayothin, B.; Cabaniss, R. A.; Blum, F. D. *Macromolecules* **2012**, *45*, 9128–9138. (c) Metin, B.; Blum, F. D. *Langmuir* **2010**, *26*, 5226–5231. (d) Fyfe, C. A.; Diaz, A. C.; Grondy, H.; Lewis, A. R.; Förster, H. *J. Am. Chem. Soc.* **2005**, *127*, 7543–7558. (e) Gould, S. L.; Tranchemontagne, D.; Yaghi, O. M.; Garcia-Garibay, M. A. *J. Am. Chem. Soc.* **2008**, *130*, 3246–3247. (f) Hepp, M. A.; Ramamurthy, V.; Corbin, D. R.; Dybowski, C. *J. Phys. Chem.* **1992**, *96*, 2629–2632.

(25) Bishop, J. J.; Davison, A.; Katcher, M. L.; Lichtenberg, D. W.; Merrill, R. E.; Smart, J. C. *J. Organomet. Chem.* **1971**, *27*, 241–249.

(26) Ackerman, J. L.; Eckman, R.; Pines, A. *Chem. Phys.* **1979**, *42*, 423–428.

(27) Seiler, P.; Dunitz, J. D. *Acta Crystallogr.* **1982**, *B38*, 1741–1745.

(28) *ACD/NMR Processor Academic Edition*, version 12.01; Advanced Chemistry Development, Inc.: Toronto, ON, Canada, www.acdlabs.com, 2010.

(29) Merckle, C.; Blümel, J. *Chem. Mater.* **2001**, *13*, 3617–3623.